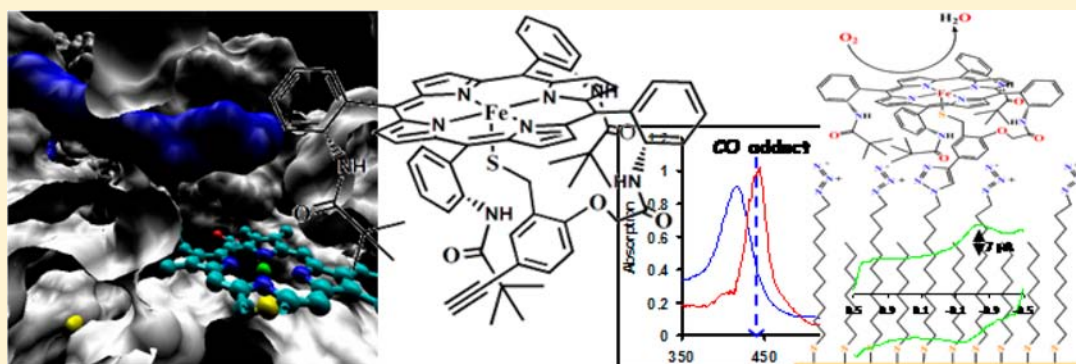


O₂ Reduction Reaction by Biologically Relevant Anionic Ligand Bound Iron Porphyrin Complexes

Subhra Samanta, Pradip Kumar Das, Sudipta Chatterjee, Kushal Sengupta, Biswajit Mondal, and Abhishek Dey*

Department of Inorganic Chemistry, Indian Association for the Cultivation of Science, Kolkata, India 700032

S Supporting Information



ABSTRACT: Iron porphyrin complex with a covalently attached thiolate ligand and another with a covalently attached phenolate ligand has been synthesized. The thiolate bound complex shows spectroscopic features characteristic of P450, including the hallmark absorption spectrum of the CO adduct. Electrocatalytic O₂ reduction by this complex, which bears a terminal alkyne group, is investigated by both physisorbing on graphite surfaces (fast electron transfer rates) and covalent attachment to azide terminated self-assembled monolayer (physiologically relevant electron transfer rates) using the terminal alkyne group. Analysis of the steady state electrochemical kinetics reveals that this catalyst can selectively reduce O₂ to H₂O with a second-order $k_{\text{cat}} \sim 10^7 \text{ M}^{-1} \text{ s}^{-1}$ at pH 7. The analogous phenolate bound iron porphyrin complex reduces O₂ with a second-order rate constant of $10^5 \text{ M}^{-1} \text{ s}^{-1}$ under the same conditions. The anionic ligand bound iron porphyrin complexes catalyze oxygen reduction reactions faster than any known synthetic heme porphyrin analogues. The kinetic parameters of O₂ reduction of the synthetic thiolate bound complex, which is devoid of any second sphere effects present in protein active sites, provide fundamental insight into the role of the protein environment in tuning the reactivity of thiolate bound iron porphyrin containing metalloenzymes.

INTRODUCTION

Cytochrome P450 (P450) represents a large family of oxygenases ubiquitous in nature. Its name is derived from the unique absorption spectrum with a maximum at 450 nm generated upon binding CO to the reduced ferrous active site.^{1,2} These enzymes have the unique ability to catalytically hydroxylate very strong C—H bonds using molecular O₂. In the course of O₂ reduction, the active site gets oxidized to generate a highly reactive intermediate known as compound I.^{3,4} This species is best described as a ferryl (Fe^{IV}=O) unit bound to a porphyrin cation radical (i.e., the dianionic porphyrin ligand is oxidized by one electron).⁵ Compound I is not unique to the P450 family. Similar species have been identified in other heme proteins involved in substrate oxidation such as peroxidases, catalases, and even in O₂ carrier proteins such as Hb and Mb.^{6–10} However, unlike other heme enzymes, which generate compound I from H₂O₂, P450 can generate compound I from molecular O₂, and the compound I thus generated is tuned to perform substrate oxidation.^{11,12}

This unique property of compound I in P450 is mostly attributed to the presence of an axial cysteine residue as opposed to histidine ligands in peroxidases.^{13–15} The cysteine residue bears a thiol side chain that coordinates the Fe atom of the heme cofactor in its anionic thiolate form.¹³ This results in a neutral resting oxidized species in P450 and an anionic reduced ferrous species. Alternatively, histidine (bearing a neutral imidazole coordinating ligand) bound heme proteins have a neutral reduced ferrous active site and a positively charged oxidized ferric active site. The axial anionic thiolate ligand of P450 exerts a “push effect” to drive the O—O bond cleavage as opposed the conventional “pull effect” associated with the peroxidases.¹⁶ The push effect of thiolate has been proposed to be responsible for several unique functional attributes of P450.¹⁷ It is proposed to lower the reduction potential of the active site, increase the pK_a of the trans axial

Received: May 24, 2013

Published: October 30, 2013



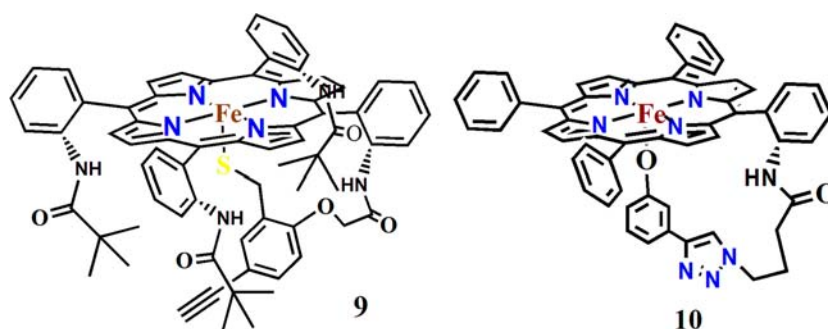


Figure 1. Schematic representation of clickable complex **9** and complex **10**.

H₂O ligand, lower the binding constants of other axial ligands, activate O—O bond cleavage, and stabilize the high oxidizing compound I species.^{18–21} Mutational studies on P450 have clearly indicated the quintessential role played by this axial thiolate ligand.^{2,5,18,22}

Naturally, understanding this phenomena that allows P450 to act as a monooxygenase utilizing O₂ and not a peroxidase utilizing H₂O₂ has been an area of major research.^{2,5,23–30} Several ferrous and ferric porphyrin complexes with axial thiolate ligands are reported which are extremely air sensitive.^{31–38} Only the ligand designed by Hirobe et al. and Naruta et al. which contain a thiolate arm attached to the porphyrin ring has been shown to be bound to the iron in both oxidized ferric and reduced ferrous forms.^{39,37,40–42} The sterically protected thiolate ligand makes these the only air-stable ferric porphyrin thiolate complexes to be reported so far. This has made several investigations possible, including substrate oxidation using peracids.^{19,36,41–43} However, to date, O₂ reduction by these thiolate bound iron porphyrin complexes have not been investigated where there are some reports of O₂ reduction by electrodes bearing cytochrome P450 enzyme.⁴⁴ On the contrary, several investigations of O₂ reduction catalyzed by iron porphyrin complexes ligated by other axial ligands are reported.⁴⁵ A comparison of physical and chemical properties of these synthetic models with those of the active site has led to deeper understanding of structure–function correlations of the enzyme active sites.^{37,45–50} As a matter of fact, several studies using these enzymes have highlighted the role of the protein environment of the enzyme active site to be a key factor in controlling its physicochemical properties.^{44,51–56} Unfortunately, such investigations using synthetic model complexes of cytochrome P450 are limited. In fact, apart from hydrogen bonding, factors affecting the reduction potential (e.g., hydrophobicity, solvation, etc.) and the O₂ activation or reduction properties of synthetic thiolate bound iron porphyrin complexes remains mostly unexplored.^{36,42,57,58} Because the P450 superfamily are the only enzymes that can catalyze hydroxylation of inert C–H bonds using an environmentally benign oxidant like O₂, understanding the details of this process is vital for mimicking this function, which has often been identified as a grand challenge in catalysis.

Heterogeneous electrocatalysis using iron porphyrin complexes immobilized on an electrode has proven to be a very convenient way of exploring the reactivities of these water insoluble complexes in an aqueous medium. This method has proved to be most rewarding in understanding the structure–function correlations of synthetic models of cytochrome *c* oxidase (CcO).^{59–62} Furthermore, the covalent immobilization on azide terminated SAM, instead of graphite surfaces, utilizing

the “click” reaction, allows tuning of the electron transfer rate from the electrode to the catalyst, which has been brilliantly exploited to understand the role of the Tyr244 residue in the active site of CcO.⁶¹ This technique has been extended to other O₂ reducing catalysts as well.^{63,64} To take advantage of this technique, a terminal alkyne group has to be inserted in the catalyst using elegant synthetic techniques.

In this paper, we report the synthesis and spectroscopic characterization of a synthetic model complex of P450 bearing a terminal alkyne group (Figure 1, (9)) with the purpose of investigating electrocatalytic oxygen reduction reactions (ORR) by a thiolate ligated iron porphyrin complex. Although there are several reports of attachment of different varieties of P450 type enzymes on electrodes, there are no reports of attachment of synthetic P450 models on electrodes.^{44,65} This air stable synthetic mimic of P450 is both physisorbed on graphite and covalently attached to an azide terminated SAM on Au electrodes using the Cu(I) catalyzed 1,3-cycloaddition of azide to alkynes; also known as the click reaction.⁶⁶ The immobilized catalyst has been characterized in situ by using surface enhanced resonance Raman spectroscopy (SERRS). The complex is air stable and hence electrocatalytic O₂ reduction of a thiolate bound heme complex has been investigated, for the first time, under both fast (immobilized on graphite surfaces) and moderate (covalently bound to SAM on Au electrodes) electron transfer conditions. For comparison, electrocatalytic O₂ reduction by a phenolate bound iron porphyrin complex has also been investigated (Figure 1, (10)). The results indicate that the presence of a thiolate complex results in the fastest reported electrocatalytic O₂ reduction rates under physiological conditions. Additionally, several physical and reactivity properties of this complex are attenuated at the protein active site by the local environment.

EXPERIMENTAL DETAILS

The necessary method and materials are given in the Supporting Information. The detailed synthetic procedures for the fragments are reported in the Supporting Information. Only the synthetic procedures for the final catalysts are described in this section.

“Clickable” Cytochrome P450 (9). To a solution of corresponding compound **8** (14 mg, 0.0107 mmol) in 10 mL of dry degassed methanol under stirring conditions in a glovebox, activated K₂CO₃ (20 mg, excess) was added, and the reaction was held for 2 h. The reaction mixture was monitored by UV spectroscopy. The reaction mixture was concentrated. Distilled dichloromethane (DCM) and water were added. The organic layer was collected, washed with brine solution, and dried over anhydrous Na₂SO₄. The solution was evaporated to dryness when a deep brown solid appeared. The crude product was recrystallized from dry DCM.

Yield: 10 mg (83%). Anal. Calcd for C₇₀H₆₃FeN₈O₅S: C, 71.00; H, 5.36; N, 9.46 Found: C, 70.64; H, 5.74; N 9.10. (¹H NMR, CDCl₃,

ppm): δ 10.32, 10.49, 12.16, 12.95, 13.11, 16.86, 56.45, 58.15, 61.69, 64.09, 80.08. IR spectra (KBr plate, cm^{-1}): 798, 1260, 1440, 1515, 1580, 1689, 2104 (free alkyne), 2963, 3419. ESI-MS (positive ion mode, acetonitrile) $m/z = 1183.8093$ (70, $[\text{M}]^+$), 1205.7839 (100, $[\text{M} + \text{Na}]^+$), 1221.7112 (40, $[\text{M} + \text{K}]^+$).

meso-Mono[*o*-5(3-phenolate-1,2,3-triazolyl)]-triphenylporphyriniron(III) (Fe^{III}(OPhP) (10). Iron phenol-functionalized porphyrin (7) (90 mg, 0.132 mmol) was dissolved in 15 mL of dry and degassed methanol in the presence of activated K_2CO_3 . The solution was stirred overnight in a glovebox. The reaction mixture was then filtered using Whatmann 40, and the filtrate was evaporated and dried using a vacuum pump inside the glovebox.

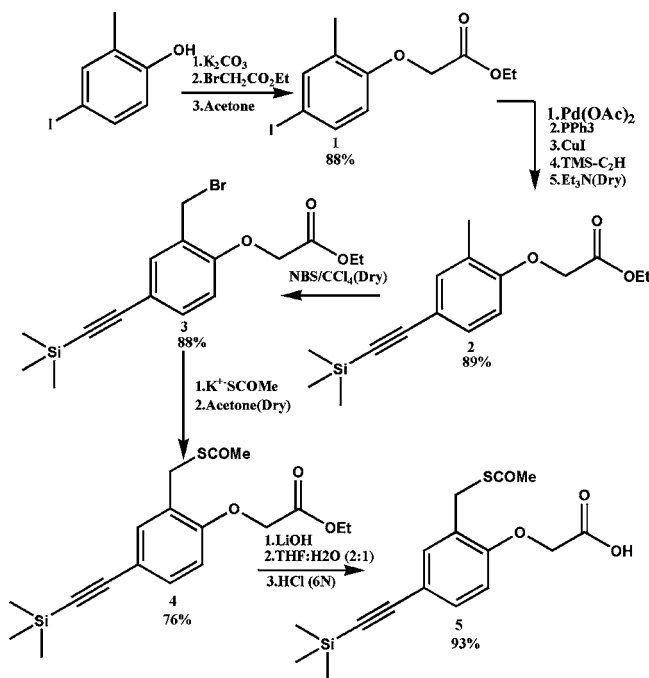
Yield: 85 mg (~94%). Anal. Calcd for $\text{C}_{57}\text{H}_{41}\text{FeN}_8\text{O}_2$: C, 73.95; H, 4.46; N, 12.10. Found: C, 72.80; H, 4.92; N, 11.68. ESI-MS (positive ion mode, acetonitrile) $m/z = 925.91$ (100, $[\text{M}]^+$). Resonance Raman (rR, in THF): $\nu_{\text{Fe-O}}$ at 573, 589 cm^{-1} , and $\nu_{\text{C-O}}$ at 1320 cm^{-1} .

RESULTS

Synthesis. Synthesis of an air stable thiolate bound iron porphyrin complex has been previously reported.⁴⁰ The same basic design (i.e., sterically protected thiolate ligand) has been maintained, and a terminal alkyne group has been introduced to allow covalent in situ attachment of this complex on to electrodes functionalized with azide linkers. This required significant modification of the previously reported synthetic approach.⁴²

Starting from 4-iodo-3-methylphenol, the thiolate ligand bearing arm for covalent attachment to the porphyrin macrocycle (5 (Lig A), Scheme 1) is synthesized in six steps.

Scheme 1. Synthetic Route of the Alkyne Protected Thiolate Ligand (5)



The bromination of the benzyl group of 4-iodo-*o*-cresol can only be performed after the substitution of the iodo group with the trimethylsilylalkyne group using Sonogashira coupling (Scheme 1). The selective hydrolysis of an ester group present in 4 in the presence of a much more labile thioester group was achieved using LiOH in a THF/ H_2O mixture. To the best of our knowledge, such selectivity is unprecedented in the literature. The trimethylsilyl protection of the alkyne group

was retained in the final product (5) to be removed after covalent attachment of this ligand to the porphyrin macrocycle.

Starting from the α_4 -*meso*-tetra(*o*-aminophenyl)porphyrin, one of the amino groups is functionalized with 5, using previously known methods (Scheme 2).⁴⁰ The monofunctionalized adduct is purified, and the remaining three amino groups are coupled to pivoyl chloride. The resultant ligand is metalated with iron using standard protocols.³³ Note that while the iron is loaded in the ferrous form (Scheme 2, 7–8), it is oxidized to the ferric form during workup. Strong acidic conditions are avoided during these steps to avoid hydrolysis of the thioester group. Both the thioacetate and the trimethylsilyl functional groups of the metalated complex are hydrolyzed under alkaline conditions in a single step under Ar atmosphere to yield the desired thiolate bound iron porphyrin complex. Once synthesized, this complex is found to be stable in air as solid for several weeks. The synthesis of the air stable phenolate bound iron porphyrin complex is detailed elsewhere (Supporting Information).

Spectroscopic and Electrochemical Investigations.

The ensuing spectroscopic and electrochemical results have been divided into two categories based on the experimental conditions. First, the spectroscopic data obtained in homogeneous conditions have been reported (section A, titled homogeneous) followed by spectroscopic and electrochemical data under heterogeneous conditions (section B, titled heterogeneous)

A. HOMOGENEOUS

A.1. Absorption Spectroscopy. The absorption spectrum of complex 9 in DCM shows a Soret band at 419 nm. The Soret shifts to 445 nm when 9 is reduced in a CO saturated solution (Figure 2, red). This is similar to the hallmark Soret band of CO adduct of cytochrome P450 at 450 nm and typical of CO adducts ferrous porphyrin complexes bearing a thiolate axial ligand.^{32,40,41} Complex 9 has several absorption bands in the visible region at 510, 577, and 647 nm, which shifts to 567, 617, and 699 nm in the CO complex (Figure 2, inset). Note that the absorption maxima of the CO complex slowly shifts to 425 nm ($t_{1/2} \sim 5$ min), suggesting protonation of the thiolate ligand under these conditions as is known for several thiolate bound heme active sites.

A.2. EPR and Resonance Raman Spectroscopy. The X-band EPR of complex 9 in MeOH at 77 K shows a $S = 1/2$ signal with g -values at 2.33, 2.21, and 1.91 (Figure 3). These are similar to those reported for the resting low spin active site of cytochrome P450 (2.45, 2.26, 1.91) as well as other thiolate ligated low spin iron porphyrin complexes (Table 1).^{37,38} Taylor analyses of these values reveal significant rhombicity typical of other thiolate coordinated low spin ferric heme complexes (Table 1) reported by Hirobe et al. and Naruta et al.⁶⁷

The rR data of complex 9 in MeOH (Figure S2, Supporting Information) obtained at room temperature (RT) shows the oxidation and spin state marker ν_4 and ν_2 bands at 1367 and 1565 cm^{-1} , respectively, indicating that it exists as a six coordinated low spin species in most solvents, consistent with the EPR data.⁶⁸

B. HETEROGENEOUS ELECTRON TRANSFER

Complex 9 is stable in air, and it contains an alkyne group. This allows for the investigation of electrochemical O_2 reduction

Scheme 2. Synthetic Route of Clickable P450 Catalyst (9)

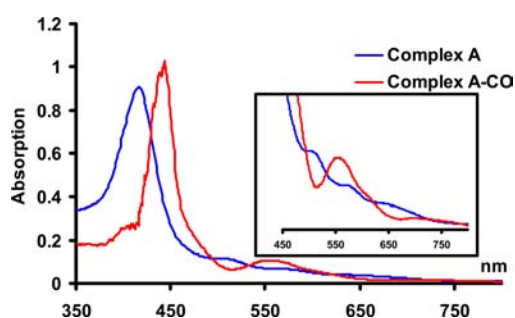
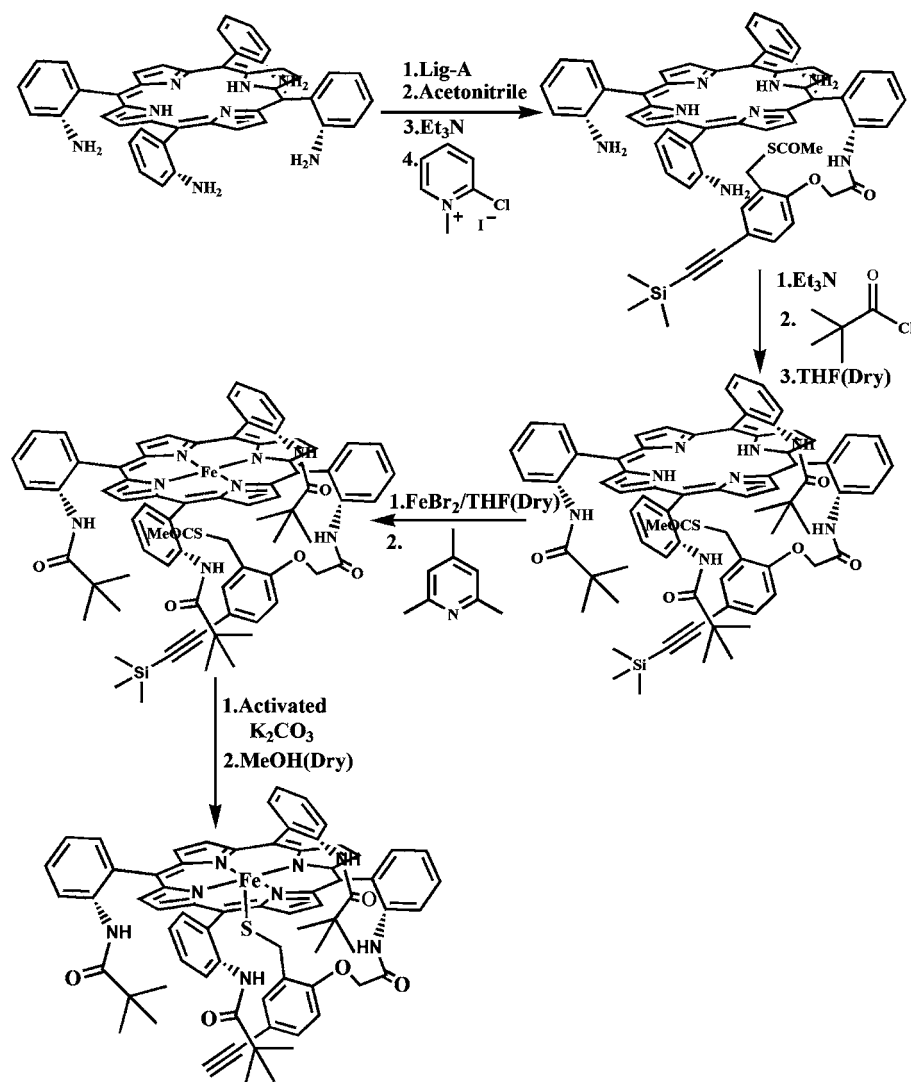


Figure 2. Spectroelectrochemistry of the clickable P450 catalyst (9) in dry DCM. Clickable p450 catalyst (9) (blue line) and clickable P450-CO bounded (red line).

properties of this catalyst physisorbed on graphite surfaces where electron transfer from the electrode to the catalyst is very fast as well as after covalent attachment to azide terminated SAM surfaces on Au electrodes where the rate of electron transfer from the electrode to the catalyst is orders of magnitude slower. Note that this is the first report of electrocatalytic O_2 reduction by a synthetic P450 analogue.

B.1. Edge-Plane Graphite (EPG): Fast Electron Transfer. The CV of complex 9 physisorbed on EPG surfaces in

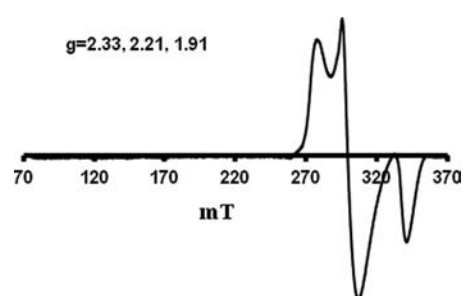


Figure 3. EPR spectroscopy of clickable P450 catalyst (9) in MeOH at 77 K.

Table 1. EPR Parameters for the Heme Thiolate Complex

	spin	g_1	g_2	g_3	V/λ
Cyt P450	1/2	2.45	2.26	1.91	4.59
Hirobe ⁴¹	1/2	2.32	2.21	1.96	6.43
Naruta ³⁷	1/2	2.33	2.21	1.96	6.55
complex 9	1/2	2.33	2.21	1.91	5.34

degassed pH 7 buffer shows a $Fe^{III/II}$ process at -0.2 V vs Ag/AgCl (Figure 4A, inset). In air saturated buffers, a large

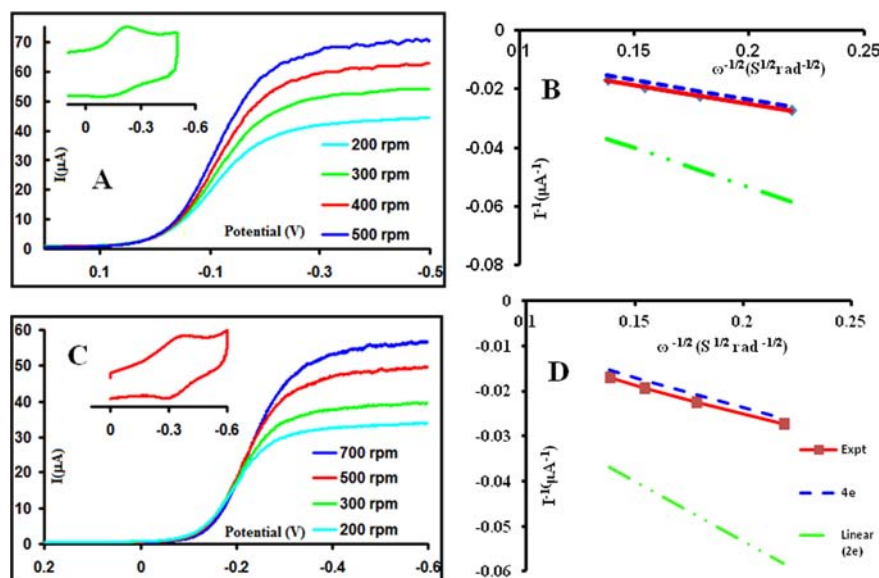


Figure 4. (A) LSV data of the clickable P450 catalyst (**9**) deposited on the EPG surface at multiple rotations in pH 7 buffer, using 100 mM KPF₆ as supporting electrolyte and Pt and Ag/AgCl as counter and reference electrode, respectively (top left), (Inset) CV of the clickable P450 catalyst (**9**) at 2 V/s scan rate in N₂ atmosphere. (B) Koutecky–Levich plot of the clickable P450 catalyst (**9**) (black bold line). The theoretical plots for the 4e[−] and 2e[−] processed are indicated by dotted and dashed lines (top right). (C) LSV data of phenolate bound iron porphyrin catalyst (**10**) (bottom left), (Inset) CV of the catalyst in N₂ atmosphere at 50 mV/s. (D) Koutecky–Levich plot of the catalyst **10** in (red bold line). The theoretical plots for the 4e[−] and 2e[−] processed are indicated by dashed blue and green lines, respectively.

electrocatalytic O₂ reduction current is observed. The onset potential of this electrocatalytic current coincides with the reduction of Fe^{III} to Fe^{II}, implying that the reduced Fe^{II} species is responsible for O₂ activation.

The kinetic parameters of O₂ reduction have been determined using RDE experiments.^{69–73} The catalytic reduction current (*i*_{cat}) has two components; the substrate diffusion controlled current (also known a Levich current (*i*_L)) and the potential dependent current (also known an kinetic current, *i*_K) such that

$$1/i_{\text{cat}} = 1/i_{\text{K}} + 1/i_{\text{L}}$$

and

$$i_{\text{L}} = 0.62nFA[\text{O}_2](D_{\text{O}_2})^{2/3}\omega^{1/2}\nu^{-1/6}$$

where *n* is the number of electrons transferred to the substrate, *A* is the macroscopic area of the disk (0.096 cm²), [O₂] is the concentration of O₂ in an air saturated buffer (0.26 mM) at 25 °C, *D*_{O₂} is the diffusion coefficient of O₂ (1.8 × 10^{−5} cm² s^{−1}) at 25 °C, ω is the angular velocity of the disk, and ν is the kinematic viscosity of the solution (0.009 cm² s^{−1}) at 25 °C.⁷⁴ Thus, the plot of 1/*i*_{cat} with the inverse of the square root of the angular rotation frequency (Figure 4B, top right) (Koutecky–Levich plot) can be used to obtain the number of electrons transferred to the substrate (*n*).⁶⁹

The RDE data of complex **9** (Figure 4A) and the phenolate bound complex (Figure 4C) indicate that a normal substrate diffusion limited current is observed below −0.4 V. The Koutecky–Levich plot of 1/*i*_{cat} vs 1/ $\omega^{1/2}$ indicates that the experimental data matches closely the theoretical plot for a 4e[−] process and not a 2e[−] process (Figure 4B,D). Thus, the synthetic P450 mimic and its phenolate analogue can reduce O₂ by 4e[−]/4H⁺ when absorbed on an EPG electrode.

The intercept of the Koutecky–Levich plot is the inverse of the kinetic current (*i*_K(*E*)^{−1}), where *i*_K(*E*) is expressed as

$$i_{\text{K}}(E) = k_{\text{cat}}nFA[\text{O}_2]\Gamma_{\text{cat}}$$

where *n* is the number of electron, [O₂] is the bulk concentration of O₂, Γ_{cat} is the surface coverage of the catalyst (obtained from the integration of the anaerobic CV data to be 2.69 × 10^{−11} mol/cm² for **9** and 5.5 × 10^{−12} mol/cm² for the phenolate analogue), *A* is the surface area of the electrode, and *k*_{cat} is the second-order rate constant for O₂ reduction.⁶⁹ With the use of this equation, the second-order rate constants for O₂ reduction by complex **9** and its phenolate analogue are determined to be (5.6 ± 1) × 10⁶ and (3.8 ± 0.1) × 10⁵ M^{−1} s^{−1}, respectively. Thus, a thiolate bound iron porphyrin can reduce O₂ at rates that are almost 2 orders of magnitude larger than the rates reported for other iron porphyrin complexes and an order of magnitude more than a phenolate bound porphyrin.⁴⁷

As discussed earlier, EPG surfaces allow for very facile electron transfer to the catalyst *k*_{ET} > 10⁵ s^{−1}. This is far from physiological conditions where the electron transfer from the reductase component to the active site varies between 4 and 1000 s^{−1} in different wild-type (WT) and mutant cytochrome P450 enzymes.^{54,75} Thus, investigation of electrocatalytic O₂ reduction is warranted under physiologically relevant slow electron transfer rates. This can be achieved by covalent attachment of complex **9** to an azide terminated thiol monolayers on Au electrodes where the rate of electron transfer can be attenuated by varying the chain length of the thiol used.⁶⁶ This has been made feasible due to the inclusion of a terminal alkyne group in the ligand. Naturally, such experiments could not be performed with the phenolate bound model, which does not bear a terminal alkyne group.

B.2. Covalent Assembled Monolayer: Moderate Electron Flux. Self-assembled monolayers bearing a mixture of azide terminated undecanethiol and octane thiol are formed on Au electrodes according to established protocols.⁶⁶ The terminal alkyne group present in complex **9** allows covalent

attachment to these azide groups on the surface of the electrode using Cu(I) catalyzed 1,3-cycloaddition of azide to alkynes (also known as the click reaction).⁶⁶ The rate of electron transfer through this monolayer is reported to be 500 s^{-1} , which is in the range of values reported for cytochrome P450 enzymes.⁷⁶ The resultant surfaces are characterized using CV and SERRS, and their O_2 reactivity are investigated.

B.2.1. Spectroscopy. Surface enhanced resonance Raman spectroscopy (SERRS) data are obtained on Ag disks covalently modified with complex **9**. The data obtained by applying a potential of 0.0 V on the disk (where all the Fe is oxidized to Fe^{III}) indicate that the complex exists mainly as a high spin species with the oxidation and spin state marker ν_4 and ν_2 vibrations at 1362 and 1552 cm^{-1} , respectively (Figure 5,

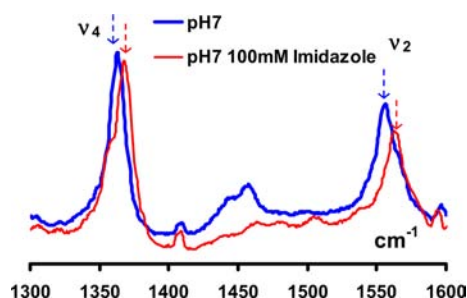


Figure 5. SERRS spectra of complex **9** covalently attached to $\text{SHC}_{11}\text{N}_3 + \text{C}_8\text{SH}$ ($\chi = 0.1$) SAM covered electrodes in the absence (blue) and presence (red) of 100 mM imidazole in pH 7 buffer at room temperature.

blue).⁶⁸ Thus, the thiolate bound ferric porphyrin complex exists mostly in the high spin state in an aqueous environment. However, in the presence of 100 mM imidazole in the buffer (Figure 5, red), the ν_4 and ν_2 vibrations shift to 1368 and 1566 cm^{-1} , respectively, indicating the conversion to a low spin state due to imidazole coordination.

B.2.2. Electrochemistry. **B.2.2.1. Anaerobic Cyclic Voltammogram.** In the absence of O_2 , complex **9** functionalized Au electrodes exhibit a $\text{Fe}^{\text{III/II}}$ process (Figure 6, red) at -0.250 mV vs Ag/AgCl (i.e., -0.05 V vs NHE). This potential is more positive than the E° reported for the P450 active site (-150 mV to -300 mV vs NHE) and may be due to structural difference and/or difference between the active site environment of the enzyme and aqueous environment of the complex

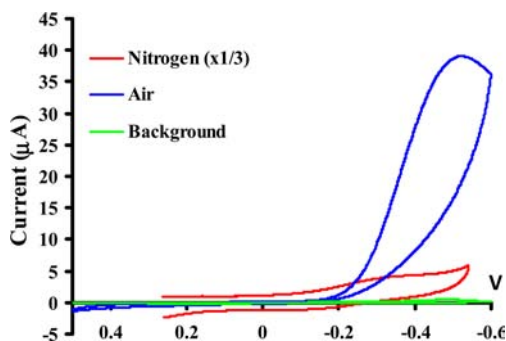


Figure 6. Cyclic voltammetry of the clickable P450 catalyst **9**, clicked on the gold wafers/disks in pH 7 buffer, using 100 mM KPF_6 as the supporting electrolyte and Pt and Ag/AgCl as the counter and reference electrode in presence of nitrogen (red) and in presence of air (blue); the green line represents the background current.

(vide infra). The integration of the current under the cathodic or anodic process is a direct measure of the number of molecules of complex **9** on the surface. This is estimated to be $(0.55 \pm 0.05) \times 10^{-12} \text{ mol/cm}^2$ of the electrode. This coverage is much lower than those obtained for the same complex adsorbed on EPG surfaces ($\sim 2.69 \times 10^{-11} \text{ mol/cm}^2$). Thus, a very dilute surface bearing these P450 mimics have been created on the SAM covered Au electrode.⁷⁷

B.2.2.2. Electrocatalytic O_2 Reduction. In the presence of O_2 , a large reduction current is observed around -0.4 V (Figure 6, blue). The onset of this current overlaps with the reduction of Fe^{III} to Fe^{II} , and it represents the electrocatalytic reduction of O_2 by the covalently attached complex **9** on the electrode. In contrast, an electrode surface covered only with the SAM alone does not show any catalytic current (Figure 6, green). The saturation of the current at negative potentials suggests that the O_2 reduction process is substrate diffusion limited at these potentials.

B.2.2.3. Partially Reduced Oxygen Species (PROS). In general, an electrocatalyst showing substrate diffusion limited currents can be characterized using rotating disk electrochemistry and Koutecky–Levich analysis as has been done for the catalyst immobilized on the EPG electrode. However, the dilute monolayer of this complex **9**, covalently attached to the electrode, is not stable enough to perform several linear sweep voltammetry (LSV) scans at varying rotation rates. Alternatively, the selectivity of O_2 reduction can be estimated by rotating ring disk electrochemistry (RRDE). In this experiment, a Pt ring that encircles the working electrode is held at a constant potential of 0.7 V (vs Ag/AgCl) while the working electrode is scanned across a potential range of interest.⁶⁹ As the potential is lowered to the region where O_2 reduction occurs, any partially reduced oxygen species (PROS, O_2^- , or H_2O_2) that may be produced by the catalyst due to incomplete O_2 reduction is diffused out toward the Pt ring due to the hydrodynamics created by the rotation of the shaft bearing the disk electrode where it is oxidized back to O_2 . This generates a reduction current on the working electrode (Figure 7, blue)

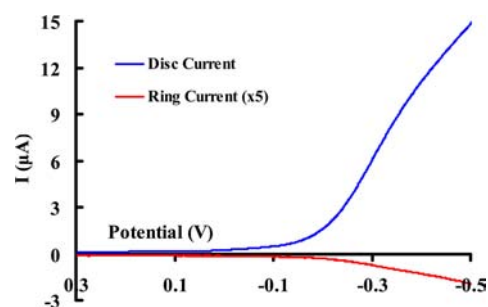
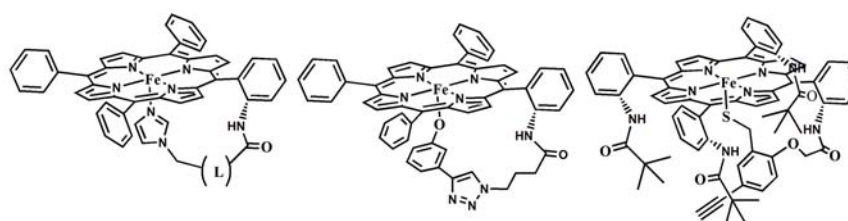


Figure 7. RRDE data of the clickable P450 catalyst, clicked on the gold disk at pH 7 buffer, at 10 mV/s scan rate, 300 rpm rotation rate using a Pt and Ag/AgCl as counter and reference electrode, respectively.

and an oxidation current (Figure 7, red) on the Pt ring. The ratio of the ring current and the catalytic current at any given potential scaled by the collection efficiency ($\sim 20\%$ in these set up) of the system yields the percentage PROS produced by the catalyst during O_2 reduction. The data on complex **9** indicates that it generates $13 \pm 1\%$ PROS during O_2 reduction. Ideally, a $2e^-$ O_2 reduction would produce 100% PROS and a $4e^-$ O_2 reduction would produce no PROS. Thus, observation of 13%



Axial Ligand	Imidazole	Phenolate	Thiolate
Spin	5/2	5/2	5/2
E° (mV vs Ag/AgCl)	-308	-300	-200
k_{cat} ($\text{M}^{-1}\text{s}^{-1}$)	5×10^4 (86)	3.8×10^5	5.6×10^6
E_{cat} (mV vs Ag/AgCl)	-400 (85, 86)	-400	-400
PROS ($k_{\text{ET}} = 10^3 \text{ s}^{-1}$)	36% (85)		13%

Figure 8. Active site models of iron porphyrins without any distal substituents. The values of imidazole bound complex are obtained from refs 85 and 86.

PROS implies $\sim 13\%$ $2e^-$ reduction of O_2 to H_2O_2 (i.e., 87% $4e^-$ O_2 reduction to H_2O).

DISCUSSION

A synthetic model of cytochrome P450 active site bearing a benzyl thiolate arm covalently attached to the porphyrin ring has been synthesized where a terminal alkyne group is introduced to allow covalent functionalization on azide terminated SAM. The synthetic procedure used utilizes selective hydrolysis of an ester group in the presence of an easily hydrolyzed thioacetate group. Such selectivity in hydrolysis has never been reported before. A final simultaneous hydrolysis of the thioester and a trimethylsilyl protecting groups yields the desired P450 synthetic model. The Soret of the $\text{Fe}^{\text{II}}-\text{CO}$ complex at 445 nm and the g -values of the solvent bound six-coordinate low spin Fe^{III} complex are consistent with the data obtained on the active site and other synthetic analogue of P450. The phenolate bound complex is synthesized in several steps (one of them involving click reaction) and the $\text{Fe}-\text{O}$ and $\text{Ph}-\text{O}$ vibrations closely match those reported for the active site of beef liver catalase.⁷⁸

Covalent attachment/immobilization of different cytochrome P450 enzymes are reported in the literature. In some cases, a $2e^-/2\text{H}^+$ reduction of O_2 to H_2O_2 has been reported, whereas in others a $4e^-/4\text{H}^+$ reduction of O_2 has been observed.^{44,79} Electron transfer (ET) rates (k_{ET}) have been proposed to alter the O_2 reduction activity of these P450 functionalized electrodes.⁵⁴ Although a close analogue of the complex (9) has been known to exhibit oxidase activity like P450,⁸⁰ here it is utilized to obtain first direct experimental O_2 electrocatalytic reduction parameters by a synthetic P450 analogue, which is free from second sphere interactions and ET rate limitations present in the protein active sites. The P450 analogue can be immobilized on EPG electrodes, which allow extremely fast electron transfer from the electrode to the complex. These electrodes catalyze selective $4e^-/4\text{H}^+$ reduction of O_2 as is reported for cytochrome P450 immobilized on HOPG electrodes where facile electron transfer to the P450 active site could be attained as well.⁵⁴ Koutecky–Levich analysis indicates that the second-order rate constant of O_2 reduction is estimated to be $(5.6 \pm 1) \times 10^6 \text{ M}^{-1} \text{ s}^{-1}$ at -200 mV , which is much faster (~ 100 times) than those reported for other iron porphyrin complexes bearing imidazole and pyridine axial

ligands to date.⁴⁷ This clearly demonstrates the role of the axial thiolate ligand in facile $\text{O}-\text{O}$ bond cleavage. In air saturated buffer (i.e., $[\text{O}_2] = 0.2 \text{ mM}$), the pseudo first-order rate constant for O_2 reduction can be estimated to be 1200 s^{-1} . Similar investigation using a phenolate bound iron porphyrin complex, immobilized on an EPG electrode, shows a second-order rate of $(3.8 \pm 0.1) \times 10^5 \text{ M}^{-1} \text{ s}^{-1}$ at -400 mV (the phenolate bound complex reduced O_2 at lower potential relative to the thiolate bound complex (Figure S4, Supporting Information)). This is about an order of magnitude slower than the thiolate bound complex.

Complex 9 has been covalently attached on azide terminated SAM on Au electrodes using click chemistry due to the incorporation of the terminal alkyl group in the ligand. The O_2 reduction catalyzed by these electrodes shows 87% $4e^-/4\text{H}^+$ reduction and $\sim 13 \pm 1\%$ $2e^-/2\text{H}^+$ reduction. Thus, under slower electron transfer, $2e^-/2\text{H}^+$ reduction of O_2 starts to prevail, which is consistent with results obtained in P450 based electrochemical bioreactors where facile electron transfer between the electrode and P450 could not be achieved.⁸¹ During electrocatalytic O_2 reduction, as the iron is reduced to its ferrous state, an initial $\text{Fe}^{\text{II}}-\text{O}_2$ adducts is formed. This adduct can either be further reduced to form a $\text{Fe}^{\text{III}}-\text{OOH}$ species ($\text{Fe}^{\text{II}}-\text{O}_2 + e^- + \text{H}^+ \rightarrow \text{Fe}^{\text{III}}-\text{OOH}$) or hydrolyzed to regenerate the oxidized ferric complex and release O_2^- in the process ($\text{Fe}^{\text{II}}-\text{O}_2 + \text{H}_2\text{O} \rightarrow \text{Fe}^{\text{III}}-\text{OH}_2 + \text{O}_2^-$). The hydrolyzed O_2^- is detected in the Pt ring in the RRDE experiments. On an EPG surface, the rate of ET is very fast and thus the formation of the $\text{Fe}^{\text{III}}-\text{OOH}$ species and further reductive cleavage of the $\text{O}-\text{O}$ bond (leading to $4e^-/4\text{H}^+$ reduction of O_2) dominated. However, when the rate of ET is lowered, the hydrolysis of the $\text{Fe}^{\text{II}}-\text{O}_2$ competes and PROS are detected in the RRDE experiments. Similar observations have been made with imidazole bound iron porphyrin complexes.⁶¹ This process of hydrolysis of the $\text{Fe}^{\text{II}}-\text{O}_2$ species formed in an enzyme active site is also known as auto-oxidation reaction.⁸² Given that the pseudo-first-order rate constant for the $4e^-/4\text{H}^+$ O_2 reduction is 1200 s^{-1} (as determined from the EPG experiments where the $4e^-/4\text{H}^+$ reduction of O_2 dominates), the rate of the competing hydrolysis reaction on SAM covered electrodes can be roughly estimated to be 13% of that (i.e., $\sim 150 \text{ s}^{-1}$) (13% of the electrocatalytic current is due to reduction of O_2 to O_2^- by the complex (i.e., auto-oxidation)) under moderate electron transfer. The auto-oxidation rate for

cytochrome P450 3A4 is reported to be 20 s^{-1} .⁸³ While the active site of P450 is buried inside the hydrophobic core of the protein, this model complex is exposed to aqueous medium. Thus the $\text{Fe}^{\text{II}}\text{-O}_2$ adduct in cytochrome P450 is protected from the aqueous environment while a putative $\text{Fe}^{\text{II}}\text{-O}_2$ adduct of this model complex likely to have formed during electrocatalytic O_2 reduction is exposed to the aqueous environment. Thus the hydrophobic active site of P450 tunes the auto-oxidation rate down ~ 7.5 times relative to a synthetic model complex which does not have a hydrophobic distal site. Note that the auto-oxidation rate in cytochrome P450 is significantly lowered in the presence of a hydrophobic substrate in the distal site (i.e., with increasing hydrophobicity of the distal site) consistent with the above proposal.^{82–84}

The rate of O_2 reduction by the thiolate and phenolate bound iron porphyrin complexes, determined here, can be compared to each other along with the results on imidazole bound iron porphyrin complexes previously reported (Figure 8).^{85,86} These complexes do not bear any distal super structure and only vary in their axial ligation, allowing unambiguous comparison of the effect of the axial ligand. The PROS data are obtained by covalently attaching the catalyst to the SAM (i.e., imposing a fixed electron transfer rate from the electrode). The k_{cat} are obtained using RDE technique with the catalyst absorbed on EPG surfaces. The results clearly show that compared to a neutral ligand, imidazole, the PROS is significantly lower in the case of the anionic thiolate ligand. Alternatively, the k_{cat} is 1 order of magnitude higher in the phenolate bound complex and 2 orders of magnitude higher in the thiolate bound complex relative to the imidazole bound complex. Note that although the $\text{Fe}^{\text{III/II}}$ potentials of the anionic ligand bound complexes are $\sim 400\text{--}500$ mV more negative relative to the neutral imidazole bound complex in a noncoordinating solvent, these potentials are very close in an aqueous medium (Figures 8 and S3, Supporting Information) as the imidazole bound complex binds an OH^- ligand to neutralize its charge.^{38,77,86} Thus, these complexes have very similar onset potentials for ORR in an aqueous medium. Furthermore, the Koutecky–Levich analyses of these complexes are performed at -400 mV vs Ag/AgCl (i.e., at the same overpotential). Thus, the increase rate of ORR likely represents the increase catalytic activity of the thiolate and phenolate bound complexes relative to the imidazole bound complex and are not affected by differences in driving force for ORR. If these results are viewed in the context of the push effect of these trans axial ligands on the mechanism of O_2 reduction, a general trend presents itself. As discussed earlier, PROS are produced due to hydrolysis of an initial $\text{Fe}^{\text{III}}\text{-O}_2^-$ adduct during O_2 reduction. Alternatively, the decay of this species leading to O–O bond cleavage involves a PCET pathway generating a $\text{Fe}^{\text{III}}\text{-OOH}$ species (known as compound 0). This process is likely to be faster when the anionic thiolate axial ligands is bound as it will increase the $\text{p}K_{\text{a}}$ of the bound O_2^- and hence reduce the production of PROS, via the competing hydrolysis reaction, relative to a neutral imidazole ligand. The k_{cat} values indicate that the O–O bond cleavage, proposed to be the rate determining step in the ORR, is also faster for both the anionic ligands relative to the neutral imidazole ligand.^{85,86} These facts are consistent with the proposal that the push effects of these ligands weaken the O–O bond causing its facile cleavage. The data clearly suggest that, of the three known ligands that bind heme in nature, the thiolate has the greatest push effect, promoting faster O–O bond cleavage.

■ ASSOCIATED CONTENT

■ Supporting Information

All the synthetic steps and the characterization data, UV–vis absorption data, and resonance Raman data. This material is available free of charge via the Internet at <http://pubs.acs.org>.

■ AUTHOR INFORMATION

Corresponding Author

*A. Dey. E-mail: icad@iacs.res.in.

Notes

The authors declare no competing financial interest.

■ ACKNOWLEDGMENTS

This work was funded by the department of science and technology, India (DST/SR/IC-35-2009) and Council for Scientific and Industrial Research (CSIR), 01(2412)10/EMr-II. S.S. acknowledges IACS Integrated Ph.D. Programme, and P.K.D., K.S., S.C., and B.M. acknowledge CSIR SRF, SRF, and SPM-JRF for fellowship.

■ REFERENCES

- (1) Omura, T. *Biochem. Biophys. Res. Commun.* **1999**, *266* (3), 690–698.
- (2) Denisov, I. G.; Makris, T. M.; Sligar, S. G.; Schlichting, I. *Chem. Rev.* **2005**, *105* (6), 2253–2278.
- (3) Davydov, R.; Macdonald, I. D. G.; Makris, T. M.; Sligar, S. G.; Hoffman, B. M. *J. Am. Chem. Soc.* **1999**, *121* (45), 10654–10655.
- (4) Newcomb, M.; Zhang, R.; Chandrasena, R. E. P.; Halgrimson, J. A.; Horner, J. H.; Makris, T. M.; Sligar, S. G. *J. Am. Chem. Soc.* **2006**, *128* (14), 4580–4581.
- (5) Shaik, S.; Kumar, D.; de Visser, S. I. P.; Altun, A.; Thiel, W. *Chem. Rev.* **2005**, *105* (6), 2279–2328.
- (6) Roman, R.; Dunford, H. B. *Biochemistry* **1972**, *11* (11), 2076–82.
- (7) Hewson, W. D.; Dunford, H. B. *Can. J. Chem.* **1975**, *53* (13), 1928–32.
- (8) Harrison, J. E.; Araiso, T.; Palcic, M. M.; Dunford, H. B. *Biochem. Biophys. Res. Commun.* **1980**, *94* (1), 34–40.
- (9) Palcic, M. M.; Rutter, R.; Araiso, T.; Hager, L. P.; Dunford, H. B. *Biochem. Biophys. Res. Commun.* **1980**, *94* (4), 1123–7.
- (10) Regelsberger, G.; Jakopitsch, C.; Engleder, M.; Rueker, F.; Peschek, G. A.; Obinger, C. *Biochemistry* **1999**, *38* (32), 10480–10488.
- (11) Rittle, J.; Green, M. T. *Science (Washington, DC, U. S.)* **2010**, *330* (6006), 933–937.
- (12) Green, M. T.; Dawson, J. H.; Gray, H. B. *Science (Washington, DC, U. S.)* **2004**, *304* (5677), 1653–1656.
- (13) Cramer, S. P.; Dawson, J. H.; Hodgson, K. O.; Hager, L. P. *J. Am. Chem. Soc.* **1978**, *100* (8), 7282–7290.
- (14) Poulos, T. L.; Finzel, B. C.; Howard, A. J. *J. Mol. Biol.* **1987**, *195* (3), 687–700.
- (15) Raag, R.; Martinis, S. A.; Sligar, S. G.; Poulos, T. L. *Science (Washington, DC, U. S.)* **1991**, *30* (48), 11420–11429.
- (16) Derat, E.; Shaik, S. J. *Phys. Chem. B* **2006**, *110* (21), 10526–10533.
- (17) Babcock, G. T.; Wikstrom, M. *Nature* **1992**, *356* (6367), 301–309.
- (18) Ogliaro, F.; de Visser, S. P.; Shaik, S. J. *Inorg. Biochem.* **2002**, *91* (4), 554–567.
- (19) Dey, A.; Okamura, T.-a.; Ueyama, N.; Hedman, B.; Hodgson, K. O.; Solomon, E. I. *J. Am. Chem. Soc.* **2005**, *127* (34), 12046–12053.
- (20) Dey, A.; Jiang, Y.; Ortiz de Montellano, P.; Hodgson, K. O.; Hedman, B.; Solomon, E. I. *J. Am. Chem. Soc.* **2009**, *131* (22), 7869–7878.
- (21) Green, M. T. *J. Am. Chem. Soc.* **1998**, *120* (41), 10772–10773.
- (22) Kumar, D.; de Visser, S. P.; Sharma, P. K.; Derat, E.; Shaik, S. *J. Biol. Inorg. Chem.* **2005**, *10* (2), 181–189.

- (23) Shaik, S.; Kumar, D.; de Visser, S. P. *J. Am. Chem. Soc.* **2008**, *130* (42), 14016–14016.
- (24) Meunier, B.; de Visser, S. I. P.; Shaik, S. *Chem. Rev.* **2004**, *104* (9), 3947–3980.
- (25) de Visser, S. P. *Biochem. Soc. Trans.* **2009**, *37* (Pt 2), 373–7.
- (26) de Visser, S. P.; Tahsini, L.; Nam, W. *Chem.–Eur. J.* **2009**, *15* (22), 5577–5587.
- (27) de Visser, S. P.; Latifi, R.; Tahsini, L.; Nam, W.-W. *Chem.–Asian J.* **2011**, *6* (2), 493–504.
- (28) Kumar, D.; Karamzadeh, B.; Sastry, G. N.; de Visser, S. P. *J. Am. Chem. Soc.* **2010**, *132* (22), 7656–7667.
- (29) de Visser, S. P. *J. Am. Chem. Soc.* **2009**, *132* (3), 1087–1097.
- (30) de Visser, S. P.; Tan, L. S. *J. Am. Chem. Soc.* **2008**, *130* (39), 12961–12974.
- (31) Sono, M.; Andersson, L. A.; Dawson, J. H. *J. Biol. Chem.* **1982**, *257* (14), 8308–8320.
- (32) Traylor, T. G.; Mincey, T. C.; Berzini, A. P. *J. Am. Chem. Soc.* **1981**, *103* (24), 7084–7089.
- (33) Collman, J. P.; Sorrell, T. N.; Hoffman, B. M. *J. Am. Chem. Soc.* **1975**, *97* (4), 913–914.
- (34) Chang, C. K.; Dolphin, D. *J. Am. Chem. Soc.* **1975**, *97* (20), 5948–5950.
- (35) Collman, J. P.; Sorrell, T. N. *J. Am. Chem. Soc.* **1975**, *97* (14), 4133–4134.
- (36) Ueyama, N.; Nishikawa, N.; Yamada, Y.; Okamura, T.-a.; Nakamura, A. *J. Am. Chem. Soc.* **1996**, *118* (50), 12826–12827.
- (37) Tani, F.; Matsu-ura, M.; Nakayama, S.; Naruta, Y. *Coord. Chem. Rev.* **2002**, *226* (1–2), 219–226.
- (38) Das, P. K.; Chatterjee, S.; Samanta, S.; Dey, A. *Inorg. Chem.* **2012**, *51*, 10704–10714.
- (39) Tani, F.; Nakayama, S.; Ichimura, M.; Nakamura, N.; Naruta, Y. *Chem. Lett.* **1999**, 729.
- (40) Higuchi, T.; Uzu, S.; Hirobe, M. *J. Am. Chem. Soc.* **1990**, *112* (19), 7051–7053.
- (41) Suzuki, N.; Higuchi, T.; Urano, Y.; Kikuchi, K.; Uekusa, H.; Ohashi, Y.; Uchida, T.; Kitagawa, T.; Nagano, T. *J. Am. Chem. Soc.* **1999**, *121* (49), 11571–11572.
- (42) Tani, F.; Matsu-ura, M.; Nakayama, S.; Ichimura, M.; Nakamura, N.; Naruta, Y. *J. Am. Chem. Soc.* **2001**, *123*, 1133.
- (43) Matsu-ura, M.; Tani, F.; Nakayama, S.; Nakamura, N.; Naruta, Y. *Angew. Chem., Int. Ed.* **2000**, *39* (11), 1989–1991.
- (44) Udit, A. K.; Hill, M. G.; Bittner, V. G.; Arnold, F. H.; Gray, H. B. *J. Am. Chem. Soc.* **2004**, *126* (33), 10218–10219.
- (45) Kim, E.; Chufan, E. E.; Kamaraj, K.; Karlin, K. D. *Chem. Rev.* **2004**, *104* (2), 1077–1134.
- (46) Enemark, J. H.; Cooney, J. J. A.; Wang, J.-J.; Holm, R. H. *Chem. Rev.* **2003**, *104* (2), 1175–1200.
- (47) Collman, J. P.; Boulatov, R.; Sunderland, C. J.; Fu, L. *Chem. Rev.* **2003**, *104* (2), 561–588.
- (48) Wasser, I. M.; de Vries, S.; Moëne-Loccoz, P.; Schröder, I.; Karlin, K. D. *Chem. Rev.* **2002**, *102* (4), 1201–1234.
- (49) Venkateswara Rao, P.; Holm, R. H. *Chem. Rev.* **2003**, *104* (2), 527–560.
- (50) Tard, C. d.; Pickett, C. J. *Chem. Rev.* **2009**, *109* (6), 2245–2274.
- (51) Sligar, S. G. *Biochemistry* **1976**, *15* (24), 5399–5406.
- (52) Das, A.; Grinkova, Y. V.; Sligar, S. G. *J. Am. Chem. Soc.* **2007**, *129* (45), 13778–13779.
- (53) Makris, T. M.; von Koenig, K.; Schlichting, I.; Sligar, S. G. *Biochemistry* **2007**, *46* (49), 14129–14140.
- (54) Whitehouse, C. J. C.; Bell, S. G.; Wong, L.-L. *Chem. Soc. Rev.* **2012**, *41*, 1218–1260.
- (55) Krishnan, S.; Abeykoon, A.; Schenkman, J. B.; Rusling, J. F. *J. Am. Chem. Soc.* **2009**, *131* (44), 16215–16224.
- (56) Udit, A. K.; Hagen, K. D.; Goldman, P. J.; Star, A.; Gillan, J. M.; Gray, H. B.; Hill, M. G. *J. Am. Chem. Soc.* **2006**, *128* (31), 10320–10325.
- (57) Kassner, R. J. *Proc. Natl. Acad. Sci. U. S. A.* **1972**, *69* (8), 2263–2267.
- (58) Matsu-ura, M.; Tani, F.; Nakayama, S.; Nakamura, N.; Naruta, Y. *Angew. Chem., Int. Ed.* **2000**, *39*, 1989.
- (59) Collman, J. P.; Fu, L. *Acc. Chem. Res.* **1999**, *32* (6), 455–463.
- (60) Collman, J. P.; Decreau, R. A.; Yan, Y. L.; Yoon, J.; Solomon, E. I. *J. Am. Chem. Soc.* **2007**, *129* (18), 5794–5795.
- (61) Collman, J. P.; Devaraj, N. K.; Decreau, R. A.; Yang, Y.; Yan, Y. L.; Ebina, W.; Eberspacher, T. A.; Chidsey, C. E. D. *Science* **2007**, *315* (5818), 1565–1568.
- (62) Collman, J. P.; Ghosh, S. *Inorg. Chem.* **2010**, *49* (13), 5798–5810.
- (63) McCrory, C. C. L.; Devadoss, A.; Ottenwaelder, X.; Lowe, R. D.; Stack, T. D. P.; Chidsey, C. E. D. *J. Am. Chem. Soc.* **2011**, *133* (11), 3696–3699.
- (64) Devadoss, A.; Chidsey, C. E. D. *J. Am. Chem. Soc.* **2007**, *129* (17), 5370–5371.
- (65) Denisov, I. G.; Sligar, S. G. *Biochim. Biophys. Acta, Gen. Subj.* **2010**, *1814*, 223–229.
- (66) Devaraj, N. K.; Decreau, R. A.; Ebina, W.; Collman, J. P.; Chidsey, C. E. D. *J. Phys. Chem. B* **2006**, *110* (32), 15955–15962.
- (67) Taylor, C. P. S. *Biochim. Biophys. Acta, Protein Struct.* **1977**, *491* (1), 137–148.
- (68) Burke, J. M.; Kincaid, J. R.; Peters, S.; Gagne, R. R.; Collman, J. P.; Spiro, T. G. *J. Am. Chem. Soc.* **1978**, *100* (19), 6083–6088.
- (69) Bard, A. J.; Faulkner, L. R. *Electrochemical Methods*; Wiley: New York, 2001.
- (70) Mu, X. H.; Schultz, F. A. *Inorg. Chem.* **1990**, *29* (16), 2877–2879.
- (71) Shi, C.; Anson, F. C. *Inorg. Chem.* **1990**, *29* (21), 4298–4305.
- (72) Shi, C.; Anson, F. C. *Inorg. Chem.* **1995**, *34* (18), 4554–4561.
- (73) Shi, C. N.; Anson, F. C. *Inorg. Chem.* **1996**, *35* (26), 7928–7931.
- (74) McCrory, C. C. L.; Devadoss, A.; Ottenwaelder, X.; Lowe, R. D.; Stack, T. D. P.; Chidsey, C. E. D. *J. Am. Chem. Soc.* **2011**, *133* (11), 3696–3699.
- (75) Daff, S. N.; Chapman, S. K.; Holt, R. A.; Govindaraj, S.; Poulos, T. L.; Munro, A. W. *Biochemistry* **1997**, *36* (45), 13816–13823.
- (76) Devaraj, N. K.; Decreau, R. A.; Ebina, W.; Collman, J. P.; Chidsey, C. E. D. *J. Phys. Chem. B* **2006**, *110*, 15955–15962.
- (77) Sengupta, K.; Chatterjee, S.; Samanta, S.; Bandyopadhyay, S.; Dey, A. *Inorg. Chem.* **2013**, *52* (4), 2000–2014.
- (78) Sharma, K. D.; Andersson, L. A.; Loehr, T. M.; Terner, J.; Goff, H. M. *J. Biol. Chem.* **1989**, *264* (22), 12772–12779.
- (79) Fleming, B. D.; Tian, Y. B.; Bell, S. G.; Wong, L.-L.; Urlacher, V.; Hill, H. A. O. *Eur. J. Biochem.* **2003**, *270*, 4082–4088.
- (80) Higuchi, T.; Shimada, K.; Maruyama, N.; Hirobe, M. *J. Am. Chem. Soc.* **1993**, *115* (16), 7551–7552.
- (81) Faulkner, K. M.; Shet, M. S.; Fisher, C. W.; Estabrook, R. W. *Proc. Natl. Acad. Sci. U. S. A.* **1995**, *92*, 7705–7709.
- (82) Denisov, I. G.; Grinkova, Y. V.; McLean, M. A.; Sligar, S. G. *J. Biol. Chem.* **2007**, *282* (37), 26865–26873.
- (83) Denisov, I. G.; Grinkova, Y. V.; Baas, B. J.; Sligar, S. G. *J. Biol. Chem.* **2006**, *281*, 23313–23318.
- (84) Li, H.; Poulos, T. L. *Nat. Struct. Biol.* **1997**, *4* (2), 140–6.
- (85) Collman, J. P.; Decreau, R. A.; Lin, H.; Hosseini, A.; Yang, Y.; Dey, A.; Eberspacher, T. A. *Proc. Natl. Acad. Sci. U. S. A.* **2009**, *106*, 7320–7323.
- (86) Boulatov, R.; Collman, J. P.; Shiryayeva, I. M.; Sunderland, C. J. *J. Am. Chem. Soc.* **2002**, *124*, 11923–11935.